Structures of the linear silicon carbides SiC_4 and SiC_6: Isotopic substitution and *Ab Initio* theory

V. D. Gordon,[a] E. S. Nathan, A. J. Apponi, M. C. McCarthy, and P. Thaddeus
Harvard-Smithsonian Center for Astrophysics, 60 Garden Street, Cambridge, Massachusetts 02138 and Division of Engineering and Applied Sciences, Harvard University, 29 Oxford Street, Cambridge, Massachusetts 02138

P. Botschwina
Institut für Physikalische Chemie der Universität Göttingen, Tammannstr, 6. D-37077 Göttingen, Germany

(Received 13 June 2000; accepted 10 July 2000)

The structures of two linear silicon carbides, SiC_4 and SiC_6, have been determined by a combination of isotopic substitution and large-scale coupled-cluster *ab initio* calculations, following detection of all of the singly substituted isotopic species in a supersonic molecular beam with a Fourier transform microwave spectrometer. Rotational constants obtained by least-squares fitting transition frequencies were used to derive experimental structures; except for those nearest the center of mass, individual bond lengths for both chains have an error of less than 0.008 Å. Accurate equilibrium structures were derived by converting the experimental rotational constants to equilibrium constants using the vibration–rotation coupling constants from coupled-cluster calculations, including connected triple substitutions. Equilibrium dipole moments and harmonic vibrational frequencies were also calculated for both chains. On the basis of the calculated vibration–rotation and *l*-type doubling constants, weak rotational satellites from a low-lying vibrational state of SiC_4 were assigned to v_6, a bending mode calculated to lie about 205 cm^{-1} above the ground state. A recommended *ab initio* equilibrium structure for SiC_8 has also been established. © *2000 American Institute of Physics.* [S0021-9606(00)01537-3]

I. INTRODUCTION

The most stable isomers of small carbon clusters are generally chains or rings, nonpolar by symmetry and thus devoid of rotational spectra. Their geometries cannot, therefore, be determined by the standard microwave technique of isotopic substitution, and for this and other reasons their structure and bonding have long been a subject of active study and debate.[1,2] The replacement of a chain's terminal carbon atom with an isovalent silicon atom yields a molecule with structure and bonding closely related to that of the pure carbon cluster but typically with a large dipole moment and a strong rotational spectrum. Experimental structures of three silicon–carbide rings—SiC_2[3] and two rhomboidal isomers of SiC_3[4,5] —have been determined by isotopic substitution, but no such structures are available for linear silicon carbides longer than SiC. The derivation of accurate structures for even a few such chains should contribute to comparative studies of similar silicon–carbon clusters and provide benchmarks for quantum-chemical calculations. Theoretical calculations[6,7] predict low-lying linear, cumulenic isomers for SiC_3 and larger silicon carbides.

Here, we report the structures of two linear silicon carbides, the previously studied SiC_4 and the recently detected SiC_6.[8] The structures of SiC_4 and SiC_6 were determined by a combination of rotational spectroscopy of the singly substituted isotopic species (done at Cambridge) and large-scale coupled-cluster ab initio calculations (done at Göttingen). The *ab initio* study of both molecules represents a considerable extension over previous work on these species.[7,9–12]

The SiC_4 and SiC_6 structures derived here (Fig. 1) are similar to those predicted for pure carbon chains, with cumulenic bonding along the entire length of the chain, including the Si–C bond. For SiC_4, in addition to lines from the normal and rare isotopic species, satellite rotational transitions were observed and assigned to several low-lying vibrationally excited states. These lines probably originate from v_6 and its overtone ($2v_6^{0,\pm 2}$), where v_6 is the second lowest-lying bending mode, calculated to lie about 205 cm^{-1} above the ground state.

II. EXPERIMENT

The rotational spectra of the normal and rare isotopic species of SiC_4 and SiC_6 were obtained by pulsed-jet Fourier transform microwave (FTM) spectroscopy.[13] In our instrument, reactive molecules are formed in the throat of a standard pulsed discharge nozzle by a low-current, high-voltage discharge through precursor gases highly diluted in an inert buffer gas. The rotational temperature of molecules in the rapidly expanding molecular beam drops to a few Kelvin by the time the gas has traveled a few centimeters downstream from the nozzle outlet, greatly enhancing the population of the lower-lying rotational levels which are of interest for structural determinations. As the beam enters the center of the spectrometer's Fabry–Perot cavity, a short pulse of microwave radiation tuned to a cavity mode macroscopically polarizes molecules with resonant rotational transitions. This

[a]Electronic mail: gordon@fas.harvard.edu

Recommended equilibrium structures (in Å) for SiC_{2n} species

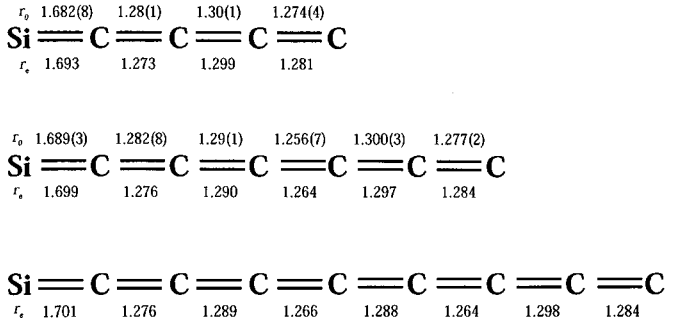

FIG. 1. Listed are the r_0 bond lengths and the mixed experimental/theoretical equilibrium structures of SiC_4 and SiC_6 and the theoretical structure of SiC_8. The 1σ errors for the experimental structures of SiC_4 and SiC_6 are given in parentheses. The equilibrium structures were derived by converting measured rotational constants to equilibrium rotational constants using the vibration–rotation coupling constants calculated from the cubic force field (see the text).

polarization then oscillates coherently at the frequency of the transition or transitions, and the subsequent free-induction decay (FID) is detected with a sensitive heterodyne receiver. The Fourier transform of the FID yields the desired line absorption power spectrum.

Fairly good predictions of the rotational constants of the isotopic species of SiC_4 and SiC_6 were made from work calculating (at the DFT-B3LYP/cc-pVDZ level of theory) equilibrium bond lengths for silicon carbide chains up to SiC_{10}.[12] Using these bond lengths, rotational constants for each singly substituted isotopic species were calculated and then scaled by the ratio of the observed B_0 to that calculated for the normal species. Such scaling consistently predicted the transition frequencies of each isotopic species to within 0.01%, i.e., less than 1 MHz at 10 GHz. Only modest frequency searches were therefore required, and misidentifications were highly unlikely.

The strongest signals of SiC_4 were obtained using a mixture of diacetylene (HC_4H,0.3%) and silane (SiH_4,0.3%) diluted in a neon buffer, a discharge voltage of 1000 V, a gas pulse of 380 μs duration, and a pressure of 2.5 kTorr behind the nozzle. Under these conditions, lines of SiC_4 were typically observed with a signal-to-noise ratio in excess of 300 in 1 min of integration. All SiC_4 singly substituted carbon-13 species could be observed in natural abundance; however, isotopic enhancement with ^{13}CO, which gave lines stronger by nearly a factor of 4, was generally employed to speed up data acquisition. For the ^{29}Si and ^{30}Si species, lines were observed in natural abundance with a signal-to-noise ratio of about 8 in about 1 min of integration. Without ^{13}CO, proportionally longer integration times were required to achieve comparable signals for each of the four ^{13}C-substituted species, i.e., about 5 min to achieve a signal-to-noise ratio of about 5–10.

Fairly good lines of SiC_6 were produced under the optimal conditions for SiC_4, but ones even stronger—by a factor of about 3—were achieved at a slightly higher discharge voltage (1300 V) and with slightly more diacetylene (0.4%) and less silane (0.1%). At best, however, the lines of SiC_6 were about six times weaker than those of SiC_4. For the two silicon isotopic species of SiC_6 in natural abundance, lines were observed with a signal-to-noise ratio of about 5 in 4 min of integration. Using ^{13}CO, the six ^{13}C-substituted species were observed at about the same signal-to-noise level in a similar integration time. Sample spectra of normal SiC_6 and two of the rare isotopic species are shown in Fig. 2.

There is compelling evidence that SiC_4, SiC_6, and their singly substituted isotopic species are the sole carriers of the assigned lines. For both molecules, the relative line strengths of the normal and rare isotopic species, as observed in natural abundance, are close to those expected. The line intensities of all the ^{13}C-containing chains increase significantly when ^{13}CO is used, and all the lines vanish when silane is removed from the discharge. None of the assigned lines diminishes in intensity when a permanent magnet is brought near the molecular beam, as expected for closed-shell molecules, and no lines were found at subharmonic intervals to indicate that we were observing molecules significantly larger or heavier than those assigned. Still further evidence of our assignments is that the centrifugal distortion constants for all of the singly substituted isotopic species of a given molecule are nearly identical.

III. SPECTROSCOPIC ANALYSIS

Both SiC_4 and SiC_6 have singlet electronic ground states and rotational transitions which are closely harmonic in frequency: $\nu_{J\rightarrow J-1}=2BJ-4DJ^3$, where J is the angular momentum quantum number for the upper rotational level and B and D are the usual rotational and centrifugal distortion constants. By fitting this expression to the rotational transitions in Tables I and II, the spectroscopic constants listed in Table III were determined. For the 16 isotopic species measured here, the rms error of each fit is comparable to the measurement uncertainties of 1–3 kHz.

Following detection and analysis of the six isotopic species of SiC_4, five additional harmonic sequences of lines less than 0.5% different in frequency from those of normal SiC_4 were subsequently observed. These lines are 20–250 times weaker than the SiC_4 main line, but each passes the same chemical and spectroscopic tests, indicating that they are carried by one or more reactive silicon-containing molecules with closed-shell electronic states and rotational constants nearly the same as that of ground state SiC_4.

These weak additional lines are most plausibly rotational satellites from the fundamental v_6 bending mode of SiC_4 and its overtone $2v_6^{0,\pm 2}$. The v_6 state is calculated in Sec. IV to be the second lowest frequency bending mode, lying about

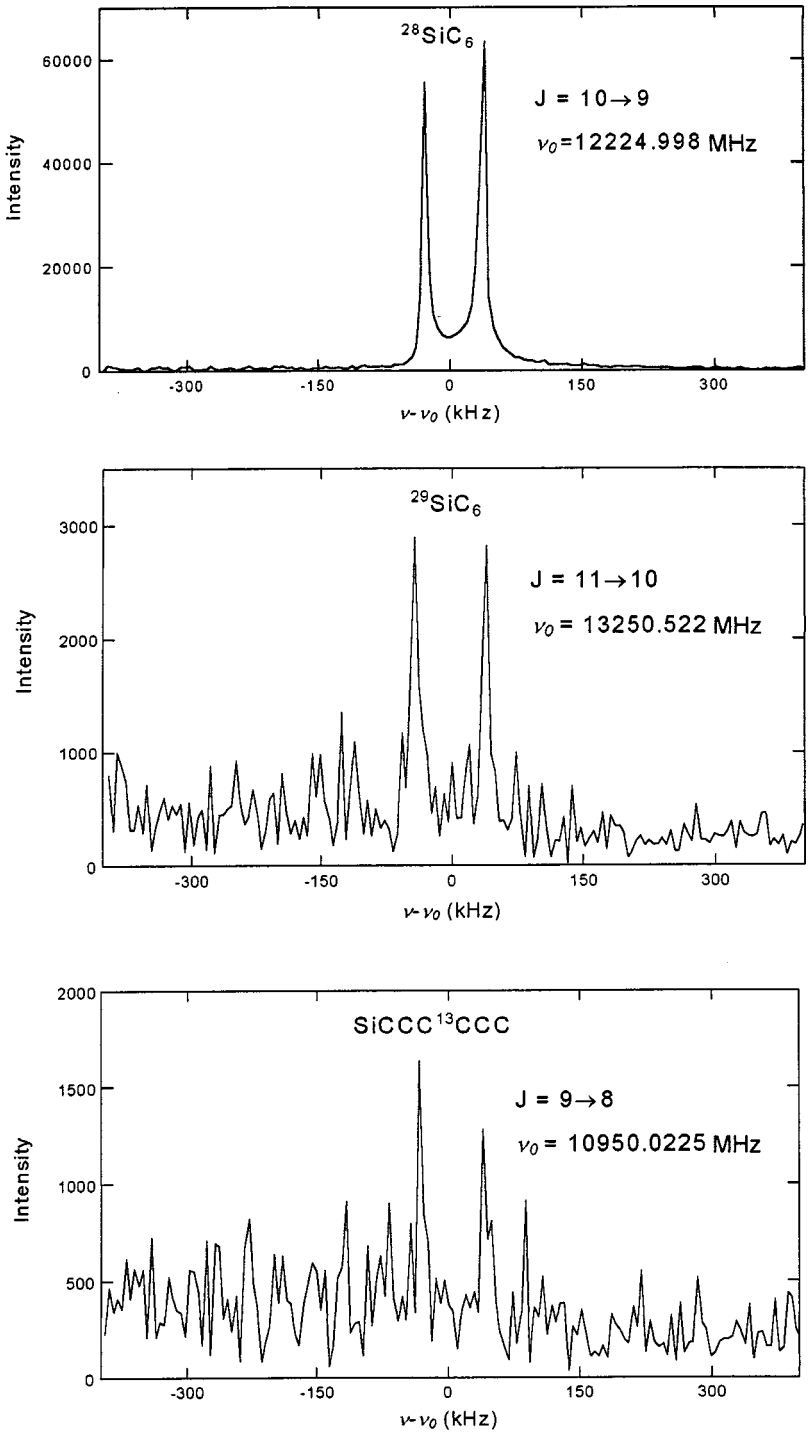

FIG. 2. Sample spectra for several isotopic species of SiC_6, including (top) normal SiC_6, (middle) $^{29}SiC_6$, and (bottom) $SiCCC^{13}CCC$, observed with ^{13}CO. Integration times are 1 min for the normal and ^{29}Si isotopic species, and 6 min for the $SiCCC^{13}CCC$ species. The double-peaked line shape results from the Doppler splitting of the fast-moving supersonic molecular beam relative to the two traveling waves that compose the confocal mode of the Fabry–Perot cavity.

205 cm^{-1} above ground. Our tentative assignment is based on three considerations. First, all of these weak extra lines lie higher in frequency than the ground-state lines; this shift rules out all rare isotopic species but not rotational satellites from bending modes, because bending tends to decrease the moment of inertia of a chain and therefore shifts the rotational lines to higher frequency. Second, differences in experimental rotational constants, $B-B(v_6)=-5.119(2)$ MHz for the $1v_6^{\pm 1}$ state and $1/2[B-B(2v_6^0)]=-4.953(2)$ MHz for the $2v_6^0$ state, both compare favorably with that expected from the calculated α_6 value of -4.953 MHz (see Table VIII): $B(v_i)=B_e-\Sigma\alpha_i(v_i+d_i/2)$, where $B(v_i)$ is the rotational constant of the ith vibration, v_i is the quantum number for the vibrational excitation, and d_i is the number of degenerate modes with the same value v_i. The experimental l-type doubling constants q_6 and q_6^J are also in excellent agreement with theory. Finally, recent millimeter-wave observations in a long-path dc glow discharge source appear to confirm our present assignments. The two lines assigned to $1v_6^{\pm 1}$ have nearly equal intensities, and both are more intense than the single line assigned to $2v_6^0$, in agreement with the relative energies of the two states. Specific searches at centimeter wavelengths for rotational satellites from v_7, the

TABLE I. Rotational transitions of the singly substituted isotopic species of SiC_4 (in MHz). Estimated experimental uncertainties (1σ) are 2 kHz. Observed minus calculated frequencies are 0–2 kHz; the best fit constants are given in Table III.

$J' \rightarrow J$	$^{28}SiC_4$[a]	$^{29}SiC_4$	$^{30}SiC_4$	$Si^{13}CCCC$	$SiC^{13}CCC$	$SiCC^{13}CC$	$SiCCC^{13}C$
3→2	9 202.629	9 061.372	8 928.148	9 192.300	9 189.856	9 095.345	8 918.687
4→3	12 270.164	12 081.826	11 904.193	12 256.394	12 253.136	12 127.131	11 891.574
5→4	15 337.695	15 102.271	14 880.229	15 320.484	15 316.410	15 158.905	14 864.460
6→5	18 405.220	18 122.716	17 856.261	18 384.567	18 379.678	18 190.665	
7→6	21 472.733	21 143.146	20 832.288	21 448.638	21 442.933	21 222.427	20 810.208
8→7	24 540.241						23 783.068

[a]Previously detected by Ohishi *et al.* (Ref. 9).

bending mode of SiC_4 that lies lowest in energy (see Sec. IV), were unsuccessful. The measured rotational satellites of SiC_4 are given in Table IV, and the effective spectroscopic constants (B, D, q, and q^J) are given in Table V.

IV. *AB INITIO* CALCULATIONS

The equilibrium bond lengths of linear SiC_4 and SiC_6 were calculated by five different methods, employing different basis sets of Dunning's correlation-consistent cc-pVnZ type.[14,15] The highest levels employed correspond to the coupled-cluster variants CCSD(T)[16] and CCSD-T.[17] In addition, CCSD,[18,19] second-order perturbation theory according to Møller and Plesset (MP2), and Hartree–Fock self-consistent field (SCF) calculations have been carried out. The largest basis set employed for SiC_4 is cc-pV5Z, which comprises 459 contracted Gaussian-type orbitals (cGTOs), with real spherical harmonics employed for the angular parts of functions with angular momentum higher than $l=1$. For SiC_6, the geometry optimizations were restricted to the cc-pVTZ and cc-pVQZ basis sets (214 and 389 cGTOs, respectively). All valence electrons were correlated in the post-Hartree–Fock calculations. Throughout, the MOLPRO98 suite of programs[20] was employed.

Calculated equilibrium bond lengths for SiC_4 are listed in Table VI, which also includes earlier results obtained by MP2 and MP3 with small basis sets.[7,9,10] As expected, only very small differences are observed between the CCSD(T) and CCSD-T results. Although the CCSD(T) values of the carbon–carbon equilibrium separations differ by less than 2%, the effects of connected triple substitutions are rather different, with R_{4e} and R_{2e} being increased by as much as 0.0131 and 0.0101 Å, respectively, while R_{3e} is elongated by only 0.0023 Å.

The complete cubic force field of SiC_4 was calculated by CCSD(T) with the cc-pVTZ and cc-pVQZ basis sets. Table VII lists the force field obtained with the larger basis set, which corresponds to an expansion of the form

$$V - V_e = \sum_{ijklmno} C_{ijklmno} \Delta R_1^i \Delta R_2^j \Delta R_3^k \Delta R_4^l \alpha^m \beta^n \gamma^o. \quad (1)$$

The angles α, β, and γ describe $SiC_{(1)}C_{(2)}$, $C_{(1)}C_{(2)}C_{(3)}$, and $C_{(2)}C_{(3)}C_{(4)}$ bending, respectively. Two angular coordinates are defined to have the same sign for a *cis*-like distortion of the nuclear framework.

The CCSD(T)/cc-pVQZ equilibrium structure from Table VI and the corresponding cubic force field from Table VII was used to calculate the spectroscopic constants given in Table VIII. Standard second-order perturbation theory in normal coordinate space was employed. The calculated harmonic stretching vibrational wave numbers are expected to be accurate to about 0.5%; the corresponding errors for the three bending vibrations should not exceed 5 cm^{-1}. The ratio $\omega_1(\text{theor.})/\nu_1(\text{exp.})$, where the experimental gas-phase value is taken from Ref. 21, is 1.023, which lies in the normal range. The lowest-energy harmonic bending vibration is predicted to lie at 88 cm^{-1} above ground.

The vibration–rotation coupling constant (α_1) for the ν_1 vibration is calculated to be 6.685 MHz for SiC_4, which is 9% below the experimental value of 7.36(29) MHz[21] but still lies within the 3σ limit. On the other hand, there is some

TABLE II. Rotational transitions of the singly substituted isotopic species of SiC_6 (in MHz). Estimated experimental uncertainties (1σ) are 2 kHz. Observed minus calculated frequencies are 0–2 kHz; fitted constants are given in Table III.

$J' \rightarrow J$	$^{28}SiC_6$	$^{29}SiC_6$	$^{30}SiC_6$	$Si^{13}CCCCCC$	$SiC^{13}CCCCC$	$SiCC^{13}CCCC$	$SiCCC^{13}CCC$	$SiCCCC^{13}CC$	$SiCCCCC^{13}C$
6→5	7 335.007								
7→6	8 557.507	8 432.163	8 313.052						
8→7	9 780.005	9 636.752	9 500.630					9 653.966	9 540.264
9→8	11 002.503	10 841.345	10 688.205	10 958.111	10 998.435	10 995.123	10 950.023	10 860.708	10 732.801
10→9	12 224.998	12 045.934	11 875.781	12 175.675	12 220.478	12 216.797	12 166.689	12 067.449	11 925.330
11→10	13 447.493	13 250.522	13 063.354	13 393.239	13 442.520	13 438.471	13 383.355	13 274.188	13 117.859
12→11	14 669.985	14 455.108	14 250.925	14 610.794		14 660.145	14 600.015	14 480.927	14 310.383
13→12	15 892.479	15 659.693	15 438.493						
14→13	17 114.968	16 864.277	16 626.063						
15→14	18 337.456	18 068.859							
16→15	19 559.942								
17→16	20 782.426								

TABLE III. Spectroscopic constants of the isotopic species of SiC_4 and SiC_6 (in MHz). Uncertainties (in parentheses) are in the last significant digit.

Molecule	B	$D\times10^6$
$^{28}SiC_4$[a]	1533.7724(2)	58(2)
$^{29}SiC_4$	1510.2298(2)	51(3)
$^{30}SiC_4$	1488.0256(2)	52(3)
$Si^{13}CCCC$	1532.0511(2)	58(3)
$SiC^{13}CCC$	1531.6439(2)	59(3)
$SiCC^{13}CC$	1515.8927(2)	51(3)
$SiCCC^{13}C$	1486.4487(2)	54(2)
$^{28}SiC_6$	611.2510(1)	5.5(2)
$^{29}SiC_6$	602.2978(1)	5.6(3)
$^{30}SiC_6$	593.7901(1)	5.4(4)
$Si^{13}CCCCCC$	608.7851(2)	7(1)
$SiC^{13}CCCCC$	611.0252(4)	7(2)
$SiCC^{13}CCCC$	610.8411(2)	6(1)
$SiCCC^{13}CCC$	608.3355(2)	5(1)
$SiCCCC^{13}CC$	603.3736(2)	5.7(8)
$SiCCCCC^{13}C$	596.2673(2)	4.3(8)

[a]Previously detected by Ohishi *et al.* (Ref. 9).

indication from experiment that the upper vibrational state involved in the ν_1 band undergoes some perturbation with another state. As discussed earlier, the calculated α_6 value agrees nicely with experiment. Previous experience indicates that the theoretical *l*-type doubling constants q_t^e are slightly underestimated when calculated from a harmonic force field, the equilibrium structure, and the atomic masses. Here, the theoretical value for q_6^e is lower than the experimental value (cf. Table V) by 4%.

The difference between equilibrium rotational constants and ground-state rotational constants, ΔB_0, was calculated from the vibration–rotation coupling constants according to

$$\Delta B_0 = B_e - B_0 \approx \tfrac{1}{2}\sum_i \alpha_i d_i \tag{2}$$

where d_i is a degeneracy factor (1 for stretching and 2 for bending modes). The resulting values are given in Table VIII. They are on the order of -4 MHz and show only a slight dependence on isotopic substitution. The equilibrium centrifugal distortion constant D_e of SiC_4 is calculated to be 46.7 Hz and thus smaller than the best available experimental ground-state value of 58.28(36) Hz[9] by 20%. Analogous CCSD(T) calculations for C_5 yield $D_e = 119.3$ Hz, to be compared with an experimental value of 163(13) Hz.[22]

Ab initio equilibrium structures, total energies, and equilibrium rotational constants for linear SiC_6 are given in Table IX. Compared to SiC_4, the silicon–carbon equilibrium separation is longer by 0.0047 Å (CCSD(T)/cc-pVQZ). For H_2CSi, analogous coupled-cluster calculations[23] yield $R_e(SiC) = 1.7171$ Å, 0.0133 Å longer than in SiC_6. The silicon–carbon bonds in SiC_4 and SiC_6 may thus be classified as strong double bonds, an inference supported by the quadratic SiC stretching force constants, which are predicted to be (in aJ Å^{-2}) 4.932(H_2CSi), 5.283(SiC_6), and 5.450(SiC_4).

TABLE IV. Rotational satellites of SiC_4 (in MHz). Estimated experimental uncertainties (1σ) are 2 kHz. Observed minus calculated frequencies are 0–2 kHz; the best fit constants are given in Table V.

$J'\rightarrow J$	$1v_6^{\pm1}$		$2v_6^{\pm0}$	$2v_6^{\pm2}$	
3→2	9230.875	9235.808	9262.063	⋯	⋯
4→3	12307.825	12314.405	12349.412	12328.470	12328.905
5→4	15384.771	15392.996	15436.752	15410.576	15411.114
6→5	18461.710	18471.578	18524.083	18492.674	18493.309
7→6	21538.639	21550.151	21611.405	⋯	⋯
48→47	147667.235	147745.800	⋯	⋯	⋯
49→48	150742.438	⋯	⋯	⋯	⋯

TABLE V. Spectroscopic constants of the rotational satellites of SiC_4 (in MHz). Uncertainties (in parentheses) are in the last significant digit.

Vibrational state	B	$D\times10^6$	q[a]	$q^J\times10^6$
$1v_6^{\pm1}$	1538.891 33(3)	61.20(7)	0.822 26(6)	−0.79(1)
$2v_6^{\pm0}$	1543.678 63(12)	69.8(16)	⋯	⋯
$2v_6^{\pm2}$	1541.087 96(13)	83.3(25)	0.002 235(7)	−28.7(2)

[a]Assumed positive.

Among the carbon–carbon bond lengths, the CCSD(T)/cc-pVQZ value for R_{4e} of SiC_6 (1.2693 Å) is remarkably short; it may be compared with the shortest equilibrium bond length in C_7 of 1.2760 Å, as obtained from analogous calculations.[24] The same sort of calculations for acetylene and ethylene yields 1.2065 Å[25] and 1.3342 Å,[26] respectively. The shortest carbon–carbon bonds of SiC_6 and C_7 thus have equilibrium bond lengths about midway between those of acetylene and ethylene.

The full cubic force field of SiC_6 has been calculated by CCSD(T) with the cc-pVTZ basis set. In addition, the 11 diagonal quadratic force constants (6 for internal stretching and 5 for bending vibrational coordinates) were obtained from CCSD(T) calculations with the large cc-pVQZ basis (389 cGTOs). Both sets of force constants were combined to produce the spectroscopic constants of Table X. One-dimensional bending potentials of SiC_6, $V(\alpha)-V(\epsilon)$, were calculated by CCSD(T)/cc-pVQZ over a wider range of angles and the results are graphically displayed in Fig. 3. All five curves are fairly steep and there is little indication that SiC_6 is a particularly floppy molecule. This view is also supported by the ratio $D_0(\text{expt.})/D_e(\text{theor.})$, which provides a reasonable measure for the degree of floppiness of a linear molecule. With the data of Tables X and III we obtain 1.17 for that ratio, even smaller than the corresponding value for SiC_4 of 1.25.

The energies of the lowest bending vibrations are predicted to be 56, 141, and 234 cm^{-1}. These vibrational states may thus be accessible to future experimental studies. According to the recent calculations of Zdetsis *et al.*,[11] the IR intensities of all bending vibrations of SiC_6 are small and so these bands will be difficult to observe by means of IR spectroscopy. The stretching vibrations ν_1 and ν_3 appear to be more promising candidates for future experimental investigation. Current work at Göttingen is devoted to accurate predictions of band positions and absolute IR intensities of stretching vibrations of SiC_6 and will be published separately.

The difference between the equilibrium and ground-state rotational constants as calculated according to Eq. (2) are

TABLE VI. *Ab initio* equilibrium bond lengths, total energies, and equilibrium rotational constants for linear SiC_4.[a]

Method	Basis	R_{1e} (Å)	R_{2e} (Å)	R_{3e} (Å)	R_{4e} (Å)	$V_e(E_h)$	B_e (MHz)
SCF	cc-pVTZ	1.6760	1.2531	1.2954	1.2518	−440.219 420	1565.6
SCF	cc-pVQZ	1.6725	1.2521	1.2952	1.2507	−440.231 673	1568.9
SCF	cc-pV5Z	1.6706	1.2520	1.2951	1.2506	−440.234 852	1570.3
MP2[b]	6-311G(d)	1.704	1.285	1.303	1.294		1508
MP2[c]	6-31G*	1.706	1.288	1.303	1.297		1504
MP2	cc-pVTZ	1.7078	1.2817	1.2998	1.2895	−440.889 856	1511.3
MP2	cc-pVQZ	1.7023	1.2789	1.2981	1.2861	−440.942 771	1518.5
MP2	cc-pV5Z	1.6995	1.2784	1.2979	1.2851	−440.962 038	1520.9
MP3[b,d]	6-31G(d)	1.689	1.275	1.303	1.278		1529
CCSD	cc-pVTZ	1.6929	1.2697	1.3016	1.2749	−440.890 026	1532.1
CCSD	cc-pVQZ	1.6870	1.2667	1.2998	1.2712	−440.934 513	1540.0
CCSD	cc-pV5Z	1.6843	1.2661	1.2993	1.2703	−440.948 151	1542.6
CCSD-T	cc-pVTZ	1.7053	1.2794	1.3039	1.2877	−440.943 446	1512.5
CCSD-T	cc-pVQZ	1.6990	1.2765	1.3019	1.2836	−440.990 893	1520.7
CCSD-T	cc-pV5Z	1.6962	1.2760	1.3016	1.2830	−441.005 541	1523.1
CCSD(T)	cc-pVTZ	1.7055	1.2797	1.3041	1.2881	−440.944 249	1511.9
CCSD(T)	cc-pVQZ	1.6991	1.2768	1.3021	1.2843	−440.991 643	1520.1
CCSD(T)	cc-pV5Z	1.6964	1.2763	1.3017	1.2834	−441.006 269	1522.6

[a]In this table and throughout the remainder of this paper, the bond lengths are numbered according to the chemical formular from left to right, starting with the silicon–carbon bond. Valence electrons are correlated in post-Hartree–Fock calculations.
[b]Reference 10.
[c]Reference 7.
[d]Reference 9.

TABLE VII. CCSD(T) cubic force field for SiC_4.[a]

i	*j*	*k*	*l*	PEF term (a.u.)	*i*	*j*	*k*	*l*	*m*	*n*	*o*	PEF term (a.u.)
A. Stretching part					B. Bending and stretch-bend part							
2	0	0	0	0.175 03	0	0	0	0	2	0	0	0.011 27
3	0	0	0	−0.152 22	0	0	0	0	0	2	0	0.058 24
0	2	0	0	0.359 65	0	0	0	0	0	0	2	0.014 18
0	3	0	0	−0.376 45	0	0	0	0	1	1	0	0.002 15
0	0	2	0	0.321 56	0	0	0	0	1	0	1	−0.000 46
0	0	3	0	−0.329 80	0	0	0	0	0	1	1	0.000 84
0	0	0	2	0.342 92	1	0	0	0	2	0	0	−0.008 13
0	0	0	3	−0.368 38	1	0	0	0	0	2	0	−0.009 66
1	1	0	0	0.015 78	1	0	0	0	0	0	2	0.003 54
1	0	1	0	−0.013 48	1	0	0	0	1	1	0	0.013 41
1	0	0	1	−0.000 37	1	0	0	0	1	0	1	−0.000 90
0	1	1	0	0.050 90	1	0	0	0	0	1	1	0.000 21
0	1	0	1	−0.024 22	0	1	0	0	2	0	0	−0.015 84
0	0	1	1	0.025 73	0	1	0	0	0	2	0	−0.039 40
2	1	0	0	−0.005 86	0	1	0	0	0	0	2	−0.000 42
1	2	0	0	−0.014 27	0	1	0	0	1	1	0	0.002 15
2	0	1	0	0.001 87	0	1	0	0	1	0	1	−0.000 14
1	0	2	0	−0.000 88	0	1	0	0	0	1	1	0.005 14
2	0	0	1	−0.003 74	0	0	1	0	2	0	0	−0.004 45
1	0	0	2	−0.002 69	0	0	1	0	0	2	0	−0.037 52
0	2	1	0	−0.023 90	0	0	1	0	0	0	2	−0.023 63
0	1	2	0	−0.028 44	0	0	1	0	1	1	0	0.002 43
0	2	0	1	−0.002 66	0	0	1	0	1	0	1	−0.000 49
0	1	0	2	0.003 65	0	0	1	0	0	1	1	−0.001 11
0	0	2	1	−0.027 11	0	0	0	1	2	0	0	0.005 77
0	0	1	2	−0.007 83	0	0	0	1	0	2	0	−0.007 23
1	1	1	0	0.007 73	0	0	0	1	0	0	2	−0.016 47
1	1	0	1	0.006 08	0	0	0	1	1	1	0	0.000 69
1	0	1	1	0.002 00	0	0	0	1	1	0	1	0.000 21
0	1	1	1	0.018 17	0	0	0	1	0	1	1	0.015 50

[a]Basis: cc-pVQZ (279 cGTOs).

TABLE VIII. Harmonic vibrational wave numbers (in cm^{-1}), vibration–rotation coupling constants (in MHz), *l*-type doubling constants (in MHz and Hz) and equilibrium quartic centrifugal constants (in Hz) for SiC_4 (CCSD(T)/cc-pVQZ).

	SiC_4	$^{29}SiC_4$	$^{30}SiC_4$	$Si^{13}CCCC$	$SiC^{13}CCC$	$SiCC^{13}CC$	$SiCCC^{13}C$
ω_1	2144	2143	2143	2134	2109	2114	2138
ω_2	1852	1852	1852	1826	1841	1828	1838
ω_3	1168	1166	1164	1150	1156	1167	1153
ω_4	571	566	561	571	570	568	565
ω_5	547	547	547	544	534	543	547
ω_6	206	206	206	204	206	202	205
ω_7	88	88	88	87	88	88	87
α_1	6.685	6.566	6.455	6.548	6.384	6.718	6.563
α_2	5.094	5.009	4.930	5.031	5.249	4.763	4.926
α_3	3.790	3.726	3.665	3.762	3.702	3.760	3.626
α_4	1.614	1.587	1.560	1.608	1.616	1.584	1.520
α_5	−2.059	−2.023	−1.990	−2.035	−2.013	−2.033	−1.998
α_6	−4.953	−4.867	−4.787	−4.841	−4.946	−4.774	−4.853
α_7	−5.562	−5.479	−5.400	−5.463	−5.490	−5.459	−5.353
ΔB_0[a]	−3.982	−3.925	−3.872	−3.863	−3.975	−3.854	−3.885
q_5^e	0.367	0.355	0.345	0.368	0.374	0.361	0.345
q_6^e	0.786	0.762	0.740	0.794	0.784	0.782	0.743
q_7^e	1.787	1.737	1.692	1.807	1.796	1.747	1.697
q_5^J	−0.048	−0.045	−0.041	−0.049	−0.051	−0.046	−0.041
q_6^J	−0.657	−0.627	−0.599	−0.659	−0.656	−0.643	−0.611
q_7^J	−3.802	−3.653	−3.515	−3.830	−3.804	−3.655	−3.511
D_e	46.7	45.4	44.2	46.5	46.6	45.7	43.5

[a] $\Delta B_0 = \frac{1}{2}\sum_i \alpha_i d_i$.

listed in Table XI. Adding these values to the experimental B_0 values from Table III produces the B_e values given in the last column of Table XI.

Equilibrium dipole moments (μ_e) listed in Table XII for SiC_4 and SiC_6 were calculated for the recommended equilibrium structures presented here (see Sec. V.B). Two flexible basis sets were employed which yield results differing by up to 0.021 D for SiC_4 and by up to 0.058 D for SiC_6. The CCSD-T and CCSD(T) calculations yield almost identical results. The CCSD(T) values obtained with the larger basis B (314 and 438 cGTOs for SiC_4 and SiC_6, respectively) are expected to be accurate to about 0.01 D. According to our recent work on SiC_8,[27] the effect of core-valence correlation on μ_e should be small. The CCSD(T) calculations with the aug-cc-pVTZ basis[15,28] yield an increase in μ_e by 1.8 D per additional C_2 unit. As for SiC_8, electron correlation effects play a significant role in the prediction of accurate μ_e values and they are substantially underestimated by CCSD. MP2 does quite a good job, apparently for the wrong reasons; this method does not consider connected triple substitutions, which seem to be very important.

V. STRUCTURES OF SiC_4 AND SiC_6

A. Experimental (r_0) structures

The goal of the present investigation is the determination of equilibrium structures (r_e), isotopically invariant geometries free of the effects of zero-point vibration. Measured ground-state rotational constants are not sufficient to determine r_e, since small but significant contributions from zero-point vibrations require that the vibration–rotation coupling constants be known as well. As a result, it is rarely feasible to determine the equilibrium structure of a polyatomic molecule solely from measurements of its isotopic species' rotational spectra; instead, various semiempirical methods must be used to determine ''near-equilibrium'' structures.[29,30]

TABLE IX. *Ab initio* equilibrium bond lengths, total energies, and equilibrium rotational constants for SiC_6.

Method	Basis	R_{1e} (Å)	R_{2e} (Å)	R_{3e} (Å)	R_{4e} (Å)	R_{5e} (Å)	R_{6e} (Å)	$V_e(E_h)$	B_e (MHz)
SCF	cc-pVTZ	1.6809	1.2525	1.2895	1.2381	1.2973	1.2513	−515.903 014	623.8
SCF	cc-pVQZ	1.6775	1.2515	1.2892	1.2370	1.2975	1.2500	−515.919 600	624.9
MP2	cc-pVTZ	1.7133	1.2863	1.2886	1.2741	1.2980	1.2929	−516.882 155	603.4
MP2	cc-pVQZ	1.7077	1.2837	1.2865	1.2715	1.2963	1.2894	−516.957 009	606.0
CCSD	cc-pVTZ	1.6978	1.2708	1.2941	1.2580	1.3021	1.2756	−516.865 065	610.9
CCSD	cc-pVQZ	1.6908	1.2681	1.2900	1.2557	1.2983	1.2722	−516.928 131	614.4
CCSD-T	cc-pVTZ	1.7102	1.2817	1.2951	1.2691	1.3029	1.2896	−516.944 295	603.9
CCSD-T	cc-pVQZ	1.7036	1.2788	1.2927	1.2662	1.3009	1.2857	−517.011 575	606.9
CCSD(T)	cc-pVTZ	1.7104	1.2818	1.2953	1.2693	1.3031	1.2900	−516.945 319	603.7
CCSD(T)	cc-pVQZ	1.7038	1.2790	1.2928	1.2665	1.3011	1.2860	−517.012 529	606.7

TABLE X. Harmonic vibrational energies (in cm^{-1}), vibration–rotation coupling constants (in MHz), *l*-type doubling constants (in MHz and Hz), and equilibrium quartic centrifugal constant (in Hz) for SiC_6.[a]

ω_1	2183	α_1	1.969	q_7^e	0.059
ω_2	2102	α_2	1.742	q_8^e	0.062
ω_3	1837	α_3	1.311	q_9^e	0.112
ω_4	1355	α_4	1.097	q_{10}^e	0.182
ω_5	879	α_5	0.751	q_{11}^e	0.448
ω_6	455	α_6	0.286	q_7^J	−0.003
ω_7	523	α_7	−0.656	q_8^J	−0.003
ω_8	497	α_8	−0.650	q_9^J	−0.020
ω_9	234	α_9	−1.218	q_{10}^J	−0.054
ω_{10}	141	α_{10}	−1.223	q_{11}^J	−0.344
ω_{11}	56	α_{11}	−1.267	D_e	4.72

[a]Spectroscopic constants are calculated using the equilibrium structure and diagonal quadratic force constants from CCSD(T) calculations with the cc-pVQZ basis set (389 cGTOs) and the remaining quadratic force constants and all cubic force constants from CCSD(T) calculations with the cc-pVTZ basis (214 cGTOs).

Experimental (r_0) structures for SiC_4 and SiC_6 were derived by a least-squares adjustment of the bond lengths in Fig. 1 to reproduce the measured rotational constants of all the singly substituted isotopic species (Table III), assuming that both molecules are linear chains—exactly the approach recently used to derive bond lengths of the long cyanopolyyne chains HC_7N, HC_9N, and $HC_{11}N$.[31] Because even the middle carbon atoms are displaced by more than 0.5 Å from the center of mass in both molecules, data for all the isotopic species were used in the fits. Except for those bonds nearest the center of mass, all individual bond lengths have been determined to an accuracy of better than 0.008 Å. The r_0 bond lengths (Table XIII) reproduce the rotational constants of the isotopic species to an accuracy of 0.02% or better, nearly ten times larger than the measurement uncertainty, but about the level where inconsistencies or anomalies attributed to zero-point motions become important.

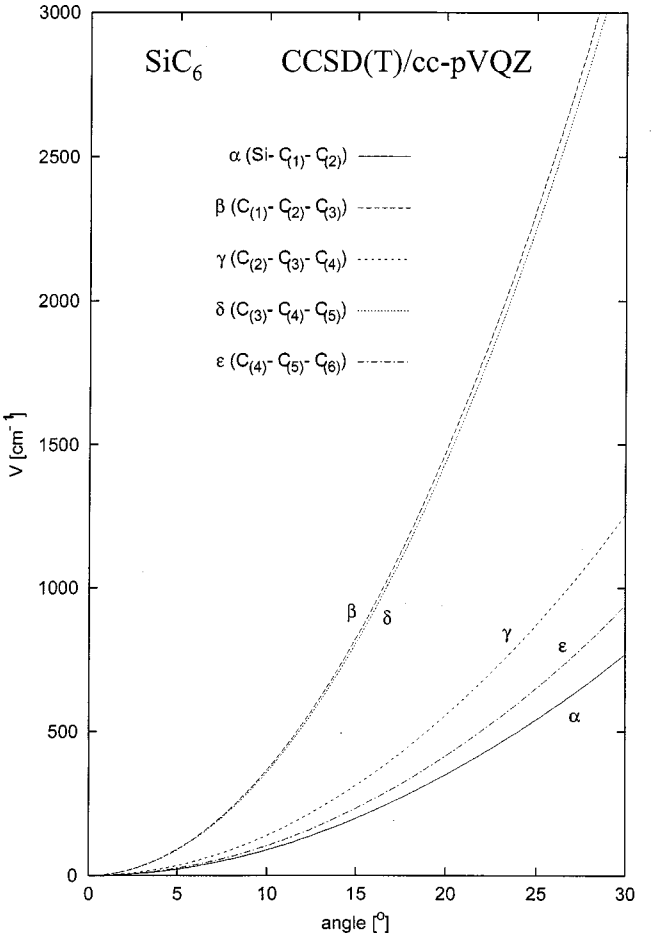

FIG. 3. Bending potentials curves (CCSD(T)/cc-pVQZ) for SiC_6.

TABLE XI. ΔB_o and B_e values for isotopomers of SiC_6.

Isotopomers	ΔB_o (MHz)	B_e (MHz)
$^{28}SiC_6$	−1.435	609.816
$^{29}SiC_6$	−1.415	600.882
$^{30}SiC_6$	−1.396	592.394
$Si^{13}CCCCCC$	−1.406	607.379
$SiC^{13}CCCCC$	−1.434	609.591
$SiCC^{13}CCCC$	−1.417	609.424
$SiCCC^{13}CCC$	−1.425	606.911
$SiCCCC^{13}CC$	−1.397	601.977
$SiCCCCC^{13}C$	−1.406	594.861

B. Mixed experimental/theoretical structures

Making use of the experimental ground-state rotational constants from Table III and the theoretical ΔB_o values from Table VIII, equilibrium rotational constants (B_e) are calculated for seven different isotopomers of SiC_4. These are converted into equilibrium moments of inertia from which equilibrium bond lengths are calculated by a least-squares fit. The results are given in column III of Table XIII; they represent our best equilibrium structure for SiC_4, with estimated uncertainties in the individual bond lengths of less than 0.001 Å. When ΔB_o values are taken from less extensive CCSD(T) calculations with the smaller cc-pVTZ basis set, we arrive at the results of column I. The values under column II correspond to an intermediate situation; for the calculation of ΔB_o values, equilibrium structure and diagonal quadratic force constants are taken from the CCSD(T) calculations with the large basis set while the remainder is taken from the CCSD(T) calculations with the cc-pVTZ basis. The differences between equilibrium structures II and III of SiC_4

TABLE XII. Calculated equilibrium dipole moments (in *D*) for SiC_4 and SiC_6.[a]

	SiC_4		SiC_6	
Method	Basis A[b]	Basis B[c]	Basis A[b]	Basis B[c]
SCF	−7.035	−7.042	−9.439	−9.500
MP2	−6.713	−6.734	−8.475	−8.533
CCSD	−7.004	−7.023	−9.312	−9.381
CCSD-T	−6.408	−6.427	−8.196	−8.248
CCSD(T)	−6.401	−6.421	−8.195	−8.249

[a]Evaluated at the recommended equilibrium structures from this work (see Section V B). The positive end of the dipole is located at the silicon site.
[b]aug-cc-pVTZ basis.
[c]aug-cc-pVQZ basis exclusive of *g* functions.

TABLE XIII. Bond lengths of SiC_4 and SiC_6.

	SiC_4				SiC_6		
		r_e[b]				r_e[b]	
Bond lengths	r_o[a]	I[c]	II[d]	III[e]	r_o[a]	I[c]	II[d]
$r(SiC_{(1)})$	1.682(8)	1.6913	1.6926	1.6928	1.689(3)	1.6980	1.6987
$r(C_{(1)}C_{(2)})$	1.280(13)	1.2735	1.2729	1.2726	1.282(8)	1.2748	1.2757
$r(C_{(2)}C_{(3)})$	1.299(10)	1.2984	1.2986	1.2986	1.291(10)	1.2910	1.2895
$r(C_{(3)}C_{(4)})$	1.274(4)	1.2797	1.2806	1.2809	1.256(7)	1.2626	1.2637
$r(C_{(4)}C_{(5)})$					1.300(3)	1.2971	1.2974
$r(C_{(5)}C_{(6)})$					1.277(2)	1.2830	1.2835

[a]Experimental (r_o) structure derived from the experimental rotational constants for the isotopic species in Table III. Statistical uncertainties in the last significant digit are given in parentheses.
[b]Mixed experimental/theoretical equilibrium structures.
[c]Using results of CCSD(T)/cc-pVTZ calculations in the calculation of ΔB_o values.
[d]Using equilibrium structure and diagonal quadratic force constants from CCSD(T)/cc-pVQZ calculations and the remainder from CCSD(T)/cc-pVTZ calculations.
[e]Using results of CCSD(T)/cc-pVQZ calculations (see Table VIII) in the calculation of ΔB_0 values.

are very small. Structure I is still quite reliable; all of its equilibrium bond lengths differ from those of structure III by less than 0.0015 Å.

Only approaches I and II (Table XIII) were feasible for SiC_6; the full cubic force field calculation for SiC_6 at the CCSD(T)/cc-pVQZ level (approach III) would be prohibitive at present. We are fairly confident that four of the carbon–carbon equilibrium bond lengths of structure II are accurate to better than 0.001 Å. The errors in the SiC and C(5)C(6) equilibrium bonds may be slightly larger, but are unlikely to exceed 0.0015 Å. Figure 1 compares the recommended equilibrium structures for SiC_4 and SiC_6; it also includes the recommended equilibrium structure for SiC_8[27] that was established at Göttingen on the basis of preliminary data for SiC_4 and SiC_6.

VI. DISCUSSION

The chemical bonding of SiC_4 is similar to that found for the isovalent Si_2C_3[32] and C_5[33] carbon clusters. In the former case, the recommended silicon–carbon equilibrium bond length (see last line of Table 1 of Ref. 32) is 1.6859 Å, 0.0069 Å smaller than the best present value for SiC_4. The recommended carbon–carbon equilibrium bond lengths in Si_2C_3 and C_5 vary between 1.2820 and 1.2893 Å, well within the range of the present C–C equilibrium bond lengths for SiC_4 and SiC_6. Small carbon clusters generally adopt linear geometries because carbon readily participates in cumulenic double bonding, but, owing to the larger atomic radius of the silicon atom, silicon clusters usually prefer single bonding over double bonding because the longer bonds reduce the sideways overlap in the perpendicular networks of π orbitals. Experimental evidence for SiC double bonds in SiC_4 and SiC_6, however, suggests that the tendency towards double bonding dominates in monosilicon carbides.

Because lines assigned to the v_6 bending state were observed in our supersonic molecular beam, it is surprising that rotational transitions from the v_7 state, lying only 88 cm^{-1} above ground, were not also found. On the basis of $v_6^{\pm 1}$ line intensities relative to those of the ground state, we estimate an effective vibrational temperature of 40–60 K, a plausible value because the electron temperature in the nozzle discharge may be 10 000 K or higher and because vibrational relaxation is typically slow. Nevertheless, the absence of the v_7 rotational satellites, weaker than the ground-state lines by a factor of 250 and weaker than v_6 satellites by a factor of 5, suggests that v_6 may be preferentially populated in our molecular beam. A possible explanation is that v_6 has a much smaller cross section than v_7 for collisional deactivation. Additional measurements at centimeter and millimeter wavelengths need to be carried out to better characterize vibrational relaxation in our molecular beam and to better constrain the vibrational temperature.

Detection of rotational satellites from at least one low-lying bending state of SiC_4 suggests that FTM spectroscopy may be a useful technique to detect rotational lines from bending modes of other linear molecules; it would be surprising if rotational satellites from other abundant chains (e.g., C_5H,H_2C_4,HC_7N, etc.) could not be found. Well-studied molecules such as HC_3N,[34] C_4H,[35] and c–C_3H_2[36] might serve as a starting point for these experiments. If rotational satellites from other carbon chains can be detected in our supersonic molecular beam, precise determinations of vibration–rotation coupling constants and *l*-type doubling constants might be useful for subsequent studies at infrared and far-infrared wavelengths.

Structural studies of other linear silicon carbides should now be feasible. Several silicon–carbon chains with an odd number of carbon atoms (e.g., SiC_3, SiC_5, and SiC_7) have recently been identified[8] using the same technique employed here. Rotational lines of at least one such chain (SiC_5) are strong enough to motivate a search for its singly substituted isotopic species. Determination of the structures of odd-*n* SiC_n chains may allow comparison of chemical bonding in triplet and singlet members of this homologous series. The rare isotopic species of SiC_8 may also be detectable with our FTM spectrometer. Under optimized conditions the strongest lines of normal SiC_8 are only four times less intense than those of SiC_6; if the line intensities of the ^{13}C isotopic species of SiC_6 can be improved by an additional factor of 3 or more by experimentation with different precursor gases and

^{13}C sources (e.g., $H^{13}C^{13}CH$), all of the singly substituted isotopic species of SiC_8 could then be found.

Radio astronomical searches for the naturally occurring isotopes of SiC_4 and SiC_6 can now be undertaken in the circumstellar shell of the evolved carbon star IRC+10216, where SiC_4[9] and other silicon–carbon chains and rings[37] have been found. With the spectroscopic constants listed in Table III, rest frequencies can be calculated to a small fraction of the linewidth in this source throughout the microwave band.

ACKNOWLEDGMENTS

We thank C. M. L. Rittby for communicating results of his quantum-chemical calculations prior to publication, and C. A. Gottlieb and W. R. M. Graham for helpful discussions. P. B. thanks Professor H.-J. Werner (University of Stuttgart) and Professor P. J. Knowles (University of Birmingham) for a copy of MOLPRO98 and the Fonds der Chemischen Industrie for financial support.

[1] W. Weltner, Jr., and R. J. Van Zee, Chem. Rev. **89**, 1713 (1989).
[2] A. Van Orden and R. J. Saykally, Chem. Rev. **98**, 2313 (1999).
[3] J. Cernicharo, M. Guélin, C. Kahane, M. Bogey, C. Demuynck, and J. L. Destombes, Astron. Astrophys. **246**, 213 (1991).
[4] A. J. Apponi, M. C. McCarthy, C. A. Gottlieb, and P. Thaddeus, J. Chem. Phys. **111**, 3911 (1999).
[5] M. C. McCarthy, A. J. Apponi, and P. Thaddeus, J. Chem. Phys. **111**, 7175 (1999).
[6] I. L. Alberts, R. S. Grev, and H. F. Schaefer, J. Chem. Phys. **93**, 5046 (1990).
[7] M. Gomei, R. Kishi, A. Nakajima, S. Iwata, and K. Kaya, J. Chem. Phys. **107**, 10051 (1997).
[8] M. C. McCarthy, A. J. Apponi, C. A. Gottlieb, and P. Thaddeus, Astrophys. J. (in press).
[9] M. Ohishi, N. Kaifu, K. Kawaguchi, A. Murakami, S. Saito, S. Yamamoto, S. Ishikawa, Y. Fujita, Y. Shiratori, and W. M. Irvine, Astrophys. J. **345**, L83 (1989).
[10] N. Moazzen-Ahmadi and F. Zerbetto, Chem. Phys. Lett. **164**, 517 (1989).
[11] A. Zdetsis, B. Engels, M. Hanrath, and S. D. Peyerimhoff, Chem. Phys. Lett. **302**, 288 (1999).
[12] X. D. Ding, S. L. Wang, C. M. L. Rittby, and W. R. M. Graham, J. Chem. Phys. **110**, 11214 (1999).
[13] M. C. McCarthy, A. J. Apponi, V. D. Gordon, C. A. Gottlieb, P. Thaddeus, T. D. Crawford, and J. F. Stanton, J. Chem. Phys. **111**, 6750 (1999).
[14] T. H. Dunning, Jr., J. Chem. Phys. **90**, 1007 (1989).
[15] D. E. Woon and T. H. Dunning, Jr., J. Chem. Phys. **98**, 1358 (1993).
[16] K. Raghavachari, G. W. Trucks, J. A. Pople, and M. Head-Gordon, Chem. Phys. Lett. **157**, 479 (1989).
[17] M. J. O. Deegan and P. J. Knowles, Chem. Phys. Lett. **227**, 321 (1994).
[18] G. D. Purvis and R. J. Bartlett, J. Chem. Phys. **76**, 1910 (1982).
[19] C. Hampel, K. Peterson, and H.-J. Werner, Chem. Phys. Lett. **190**, 1 (1992).
[20] MOLPRO98 is a package of *ab initio* programs written by H.-J. Werner and P. J. Knowles, with contributions from J. Almløf, R. D. Amos, A. Berning *et al.*
[21] A. Van Orden, R. A. Provencal, T. F. Giesen, and R. J. Saykally, Chem. Phys. Lett. **237**, 77 (1995).
[22] N. Moazzen-Ahmadi, A. R. W. McKellar, and T. Amano, J. Chem. Phys. **91**, 2140 (1989).
[23] P. Botschwina, unpublished results.
[24] P. Botschwina, Theor. Chem. Acc. **104**, 160 (2000).
[25] J. M. L. Martin, T. J. Lee, and P. R. Taylor, J. Chem. Phys. **108**, 676 (1998).
[26] J. M. L. Martin and P. R. Taylor, Chem. Phys. Lett. **248**, 336 (1996).
[27] P. Botschwina, B. Schulz, R. Oswald, and H. Stoll, Z. Phys. Chem. (Munich) **214**, 797 (2000).
[28] R. A. Kendall, T. H. Dunning, Jr., and R. J. Harrison, J. Chem. Phys. **96**, 6796 (1992).
[29] M. D. Harmony, Acc. Chem. Res. **25**, 321 (1992).
[30] J. K. G. Watson, A. Roytburg, and W. Ulrich, J. Mol. Spectrosc. **196**, 102 (1999).
[31] M. C. McCarthy, E. S. Levine, A. J. Apponi, and P. Thaddeus, J. Mol. Spectrosc. **203**, 75 (2000).
[32] P. Botschwina, J. Mol. Spectrosc. **198**, 192 (1999).
[33] P. Botschwina, J. Chem. Phys. **101**, 853 (1994).
[34] K. M. T. Yamada and R. A. Creswell, J. Mol. Spectrosc. **116**, 384 (1986).
[35] S. Yamamoto, S. Saito, M. Guélin, J. Cernicharo, H. Suzuki, and M. Ohishi, Astrophys. J. **323**, L149 (1987).
[36] R. Mollaaghababa, C. A. Gottlieb, J.-M. Vrtilek, and P. Thaddeus, J. Chem. Phys. **99**, 890 (1993).
[37] A. J. Apponi, M. C. McCarthy, C. A. Gottlieb, and P. Thaddeus, Astrophys. J. **516**, L103 (1999).